Translational Oncology 24 (2022) 101498

Contents lists available at ScienceDirect

Translational Oncology

journal homepage: www.elsevier.com/locate/tranon

Original Research

Anti-tumor effect of aquaporin 3 monoclonal antibody on syngeneic mouse tumor model

Manami Tanaka [a], Anmi Ito [a], Seiji Shiozawa [b,c], Mariko Hara-Chikuma [a,*]

[a] Department of Pharmacology, School of Medicine, Keio University, 35 Shinano-machi, Shinjuku-ku, Tokyo 160-8582, Japan
[b] Center for Integrated Medical Research, School of Medicine, Keio University,160-8582, Japan
[c] Institute of Animal Experimentation, School of Medicine, Kurume University, 830-0011, Japan

ARTICLE INFO

Keywords:
Cancer therapy
Aquaporin 3
Tumor-associated macrophage
Tumor microenvironment
Macrophage

ABSTRACT

Aquaporin-3 (AQP3), a water channel protein, has been found to be involved in cancer progression via water and small molecule transport function. However, drug development targeting AQP3 has not yet begun.

Here, we showed that a recently established anti-AQP3 monoclonal antibody (mAb) suppresses tumor growth in allograft mouse colorectal tumor models produced using CT26 or MC38 cancer cells. Administration of the anti-AQP3 mAb to BALB/c mice with transplanted CT26 cells increased the M1/M2 ratio of tumor-associated macrophages (TAM) and improved the mitochondrial function of T cells in the tumor microenvironment (TME). Administration of anti-AQP3 mAb also restored the TAM-induced decrease in T cell proliferation. Macrophage depletion in wild-type mice counteracted the antitumor effect of anti-AQP3 mAb in the mouse tumor model, suggesting that one of the primary targets of anti-AQP3 mAb is macrophages. In *in vitro* studies using mice bone marrow monocytes and human monocyte THP-1 cells, anti-AQP3 mAb attenuated carcinoma cell-mediated polarization of monocytes into M2-like TAMs.

These data suggest that anti-AQP3 mAb suppresses tumor growth by attenuating immunosuppressive M2-like TAMs, which in turn maintains the antitumor function of T cells in the TME. Thus, the anti-AQP3 mAb is a potential cancer therapy that functions by targeting TAMs.

Introduction

Knowledge in the molecular mechanisms and pathophysiology of human cancer has resulted in the development of many targeted drugs. However, cancer remains the leading cause of death worldwide. Cancer progression depends on processes occurring in the tumor microenvironment (TME), which consists of carcinoma, stromal, and infiltrating immune cells. The cross-talk that occurs between carcinoma and immune cells (which includes tumor-associated macrophages, TAMs) contributes to tumor growth, metastasis, and tumor response to therapy [1–4].

Macrophages are key regulators of tissue homeostasis. They were originally classified according to the spectrum of their responses, *e.g.*, M1 macrophage are pro-inflammatory, whereas M2 macrophages are anti-inflammatory [5,6]. In the TME, M2-like TAMs promote tumors in several ways, *e.g.*, they increase the rates of proliferation and metastasis of cancer cells, angiogenesis, and recurrence; in contrast, M1-like TAMs suppress tumors through cytotoxic responses or high levels of phagocytosis [7–10]. M2-like TAMs also play a role in a cancer's resistance to conventional antitumor therapies (*i.e.*, chemotherapy or radiotherapy) as well as in reducing the effectiveness of new immunotherapies, such as immune checkpoint inhibitor-based therapies targeting programmed death 1 (PD1) [11,12]. Hence, recent studies have suggested that TAMs are a key target for improving the efficacy of immunotherapies [8,13]. Thus, some TAM-targeted antitumor therapies currently under development involve macrophage depletion, inhibition of macrophage recruitment, and macrophage reprogramming [8,14,15].

Aquaporins are a family of water- and small molecule-transporting proteins, and aquaporin-3 (AQP3) is involved in various cellular functions, such as cell proliferation and migration, via AQP3-mediated

Abbreviations: AQP3, aquaporin 3; mAb, monoclonal antibody; TAM, tumor-associated macrophages; TME, tumor microenvironment; BM, bone marrow; CAF, cancer-associated fibroblast; LPS, lipopolysaccharide; OCR, oxygen consumption rate; Arg1, Arginase 1; FACS, fluorescence-activated cell sorting; MACS, magnetic activated cell sorting; TGI, tumor growth inhibition.

* Corresponding author.
E-mail address: haramari@kuhp.kyoto-u.ac.jp (M. Hara-Chikuma).

https://doi.org/10.1016/j.tranon.2022.101498
Received 11 April 2022; Received in revised form 13 July 2022; Accepted 25 July 2022

water, glycerol, or hydrogen peroxide (H_2O_2) transport [16–19]. We previously reported that AQP3 expression is involved in inflammatory diseases such as psoriasis, allergic diseases, and liver fibrosis, and in pathogenesis and progression of several cancers [20–26]. Specifically, AQP3-mediated increase in intracellular H_2O_2 concentration acts as a second messenger in cell signaling processes that involve NF-κB or PTEN, which are factors that contribute to inflammation, cell proliferation, and cell migration. We recently developed a neutralizing anti-AQP3 monoclonal antibody (mAb) that binds to the extracellular domain of AQP3, in an effort to develop a liver fibrosis therapy that targets AQP3 [24]. Anti-AQP3 mAbs inhibit AQP3-facilitated H_2O_2 and glycerol transport, thus suppressing H_2O_2-facilitated NF-kB activation in macrophages. The administration of anti-AQP3 mAb to an experimental mouse model prevented liver injury by inhibiting inflammation, oxidative stress, and macrophage activation. We speculate that by targeting macrophages, anti-AQP3 mAbs may be an effective therapy against diseases such as cancer.

The present study examines the effectiveness of anti-AQP3 mAbs in suppressing the progression of cancer. We performed experiments on murine syngeneic tumor models to show that anti-AQP3 mAbs suppress cancer growth *in vivo* through regulating the immunosuppressive function.

Materials and methods

Mice

C57BL/6 and BALB/c mice were purchased from Japan SLC, Inc. AQP9$^{-/-}$ mice were generated via targeted gene disruption as described previously [27]. AQP3 knockout mice were generated in-house by genome editing. Briefly, exons 2–4 were deleted by the Alt-R® CRISPR-Cas9 system (Integrated DNA Technologies Inc.) using the following two mixed guide RNAs (gRNAs); AQP3_crRNA_5′: TGGATGTCATTTAACCACCT, AQP3_crRNA_3′: AACGCCACCACCATGTTCTG. Cas9-gRNA complexes were introduced into fertilized eggs of C57BL/6 mice by electroporation method. The next day, genome edited 2-cell embryos were transferred into the oviducts of pseudo-pregnant surrogate mothers, and pups were obtained. After weaning, genotyping by PCR was performed using the tail tip genomic DNA. The primer pair used were as follows for AQP3-; 5′- GATACGCAGACATTTCTCCATGC, 5′-CGATGGCCAGTACACACACA

ATA, and for wild-type; 5′-AGACAACGCCACCACCATGTTCTG, 5′-TAGGGGAAA

GAAACGAGTTGGGC, and 5′-CTCTATGGCTTCTGAGGCGGAAG (Supplementary Fig. 5).

All animal experiments were approved by the President of Keio University, following the consideration by the Institutional Animal Care and Use Committee of Keio University (approval no: 16075) and by Genetic Modification Safety Committee, Keio University School of Medicine (approval no.28-029), and were carried out in accordance with institutional procedures, national guidelines, and the relevant national laws on the protection of animals.

Development of an anti-AQP3 antibody

Anti-mouse monoclonal AQP3 antibody was developed as described previously [24]. In brief, an oligopeptide was synthesized consisting of the amino acid sequence corresponding to positions 148–157 of the mouse/human AQP3 polypeptide. A C57BL/6 mouse was immunized using the synthetic peptide together with mouse AQP3-overexpressing CHO-K1 cells and an adjuvant. The immune cells from the immunized mouse were obtained, and an antibody gene phage library was constructed [28]. The selected AQP3-binding colonies were made into IgG immunoglobulins to give anti-AQP3 mAb.

Cell culture and cell growth assay

CT26 (Riken BRC cell bank, JAPAN) and THP-1 (ATCC) were grown in RPMI medium containing 10% FBS and penicillin-streptomycin (100 u/ml and 100 μg/ml). MC38 (kindly provided by Dr. James P. Allison, Memorial Sloan Kettering Cancer Center, New York), HaCaT cells (Cell Line Service, Germany), and MDA-MB231 (ATCC) were grown in Dulbecco's modified Eagle medium containing 10% FBS and penicillin–streptomycin. To assess cell growth, cell number was quantified by CellTiter-Glo assay according to manufacturer's instructions (Promega).

Syngeneic tumor models

6–8-week-old mice were injected with CT26 or MC38 colon carcinoma cells (4×10^6 cells in a 100 μl PBS) by intradermally into the right flank of mice. Monotherapy with the anti-AQP3 antibody was started when the tumor size reached 50–60 mm^3 (around day 6). Monoclonal anti-AQP3 antibody [24] or a matched isotype control (mouse IgG2a isotype control, clone #C1.18.4, BioXcell) were injected intraperitoneally (i.p.) (12.5 mg/kg weight) every 3 to 4 days. Tumor size was measured with digital caliper and calculated by the following formula: volume = ($width^2$ x length)/2. To deplete macrophages in some experiments, mice were intravenously administrated chlodronate liposome (10 μl/g weight, Xygieia Bioscience) every four days during assay.

Flow cytometry analysis

Tumor tissues were minced and digested with a mixture of liberase (25 μg/ml; Roche) and DNase I (10 μg/ml, Sigma). Spleen or lymph node were minced to collect single cells. Single cell suspensions were stained with monoclonal antibodies against CD45, CD3, CD4, CD8, CD44, CD62L, CD69, CD11B, F4/80, MHCII, CD206, Ly6G (Gr-1), Ly6C, B220, CD80, CD86, DX5 (eBioscience, San Diego, CA), and MitoTracker (Thermo Fisher). The samples were analyzed using the flow cytometry CytoFLEX (Beckman Coulter Life sciences, Brea, CA).

Bone marrow derived macrophage preparation

Single cell suspensions of bone marrow cells were collected from femur and tibia. Cells were cultured in RPMI 1640 (Invitrogen) containing 10 ng/ml GM-CSF (R&D), 10% FBS, 50 μM 2-mercaptoethanol, 2 mM L-glutamine, 25 mM HEPES, 1 mM nonessential amino acids, 1 mM sodium pyruvate, penicillin-streptomycin (100 u/ml and 100 μg/ml) for at least 6 days. More than 90% of cultured cells were confirmed as macrophages using FACS analysis [24]. Macrophages were incubated with LPS (1 ng/ml) and IFN-g (10 ng/ml) for M1, or with IL-4 (10 ng/ml) for M2 polarization.

Monocytes and CAF preparation, and co-culture

Single cell suspensions of bone marrow cells were collected from femur and tibia. The cell suspensions were stained with Monocyte Isolation Kit (#130-100-629, Miltenyi Biotec) and sorted monocytes by MACS Columns and separator according to manufacturer's instructions.

Tumor tissues were minced and digested with a mixture of liberase (25 μg/ml; Roche) and DNase I (10 μg/ml, Sigma). Cell suspensions were stained with Tumor-Associated Fibroblast Isolation Kit (#130-116-474, Miltenyi Biotec) and sorted CAF by MACS Columns and separator according to manufacturer's instructions.

Isolated CAF or CT26 colon cancer cells were co-cultured with monocytes using transwell membrane (0.4 μm pore, 662641, GIBCO).

RNA extraction and real-time quantitative RT-PCR

Total RNA was extracted using TRIZOL (Invitrogen). The cDNA was

reverse transcribed from total RNA using the Prime Script RT reagent kit (Takara Bio, Otsu, Japan). Quantitative RT-PCR was performed using SYBR Green I (Takara Bio) and StepOne Plus real-time PCR apparatus (Thermo Fisher).

Measurement of oxygen consumption rate

The oxygen consumption rate (OCR) of T cells was measured using an XF24 Extracellular Flux analyzer (Seahorse Biosciences). Briefly, sorted T cells from draining lymph nodes were seeded in an XF24 cell culture microplate. Mitochondrial oxygen consumption was measured with an XFe Cell MitoStress Test, in which OCR were measured after sequential addition of oligomycin, FCCP, and rotenone/antimycin A.

In vivo monocyte transfer

BALB/c mice were intradermally injected with CT26 cells and administrated anti-AQP3 mAb or control IgG by intraperitoneally as shown in Fig. 5A. Naïve monocytes were isolated from bone marrow cell suspension by MACS separator, as described above. The monocytes were stained with Qtracker Cell Labeling kit (Thermo Fisher), and transferred into CT26 tumor tissue. Tumor tissues were digested and stained with antibodies, and analyzed using the flow cytometry CytoFLEX (Beckman Coulter Life sciences).

In vitro T cell proliferation assay

BALB/c mice were intradermally injected with CT26 cells and administrated anti-AQP3 mAb or control IgG by intraperitoneally as shown in Fig. 5B. Tumor tissues were digested and isolated $CD11B^+$ TAMs with CD11B MicroBeads and MACS separator (Miltenyi Biotec). Naïve T cells were isolated from mice spleen with Pan T Cell Isolation kit and MACS separator, and stain with CSFE cell proliferation kit (Thermo Fisher). T cells were co-cultured with $CD11B^+$ cells in the presence or absence of anti-CD3/28 beads (Dynabeads Mouse T-Activator CD3/28, Gibco) and IL-2 (30 U/ml, Peprotech) according to manufacturer's instructions. After co-culture for 3 days, collecting T cells were stained with anti-CD4, anti-CD8, and SYTOX blue dead cell staining (Thermo Fisher), and analyzed by the flow cytometry CytoFLEX (Beckman Coulter Life sciences).

Statistical analysis

Statistical analysis was performed using the two-tailed Student's t-test, one way or two-way ANOVA by GraphPad Prism8.

Results

Anti-AQP3 mAbs suppress tumor growth in a syngeneic mouse tumor model

The antitumor effect of anti-AQP3 mAbs was tested on two murine syngeneic tumor models with CT26 and MC38 colonic cancer cells. These mice models are known to be highly immunogenic tumor models [29–31]. Mice bearing cancer cells were treated with an anti-AQP3 mAb or control-IgG every 3 to 4 days. Administration of anti-AQP3 mAb significantly suppressed tumor growth compared with control IgG treatment (Fig. 1A, Supplementary Fig. 1A). The treatment of BALB/c mice with CT26 tumors with anti-AQP3 mAb resulted in more tumor growth inhibition (TGI) than that in C57BL/6 mice with MC38 tumors (TGI at day 22 for BALB/C with CT26, 71%; for C57BL/6 with MC38, 47%). No signs of toxicity or weight loss were observed in any of the treatment groups (Supplementary Fig. 1B, C).

AQP3 is expressed in a variety of cancer cells, including cutaneous and breast cancers [18,26,25]. We have verified, via real time RT-PCR analysis, that CT26 and MC38 cells express little AQP3 (data not shown). Accordingly, FACS analysis show that anti-AQP3 mAbs do not bind to CT26 or MC38 cells, whereas specific mAb binding to endogenous AQP3 in human keratinocyte HaCaT cells was observed (Fig. 1B, Supplementary Fig. 1D). We determined the effect of anti-AQP3 mAbs on cancer cell growth *in vitro*. Supplementing anti-AQP3 mAbs to the culture medium did not affect cancer cell growth, suggesting that these mAbs have little direct effect on cancer cells (Fig. 1C).

AQP3 is expressed in various immune cells, such as T cells, dendritic cells, monocytes, and macrophages [32,21,24]. We determined the binding of anti-AQP3 mAb to immune cells derived from the spleen and bone marrow of BALB/c and C57BL/6 mice, which are recipient strains for CT26 and MC38 cells, respectively. FACS analysis show that anti-AQP3 mAbs bind to macrophages, T cells, and dendritic cells (Fig. 1D; Supplementary Fig. 1E). Additionally, anti-AQP3 mAbs also bound to tumor-infiltrating immune cells, *i.e.*, macrophages and T cells collected from CT26 and MC38 transplanted tumor tissues, whereas little binding occurred with cancer cells (Supplementary Fig. 2A).

AQP9 is a close homolog to AQP3, and it is expressed in various immune cells such as macrophages and neutrophils [32–34]. Thus, we compared the binding specificities of anti-AQP3 mAb to AQP3 and AQP9 knockout cells. FACS analysis showed that anti-AQP3 mAb bind specifically to AQP3 (Fig. 1E; Supplementary Fig. 1F). Overall, these results suggest that the *in vivo* effect of anti-AQP3 mAb on tumor growth occurs via immune cells such as macrophages and T cells; and the antibodies have no direct effect on cancer cells.

Administration of anti-AQP3 mAb alters intratumoral macrophage profile and T cell activation

Tumor-infiltrating immune cells, including T cells and macrophages, are able to modulate cancer progression by affecting cancer cell growth, angiogenesis, or metastasis [35–37]. To elucidate the mechanism used by anti-AQP3 mAbs to suppress tumor growth, we analyzed tumor-infiltrating immune cells in transplanted CT26 tumor tissue by flow cytometry. The ratios of T cells ($CD4^+$ or $CD8^+$) and $CD11C^+$cells relative to $CD45^+$ immune cells in tumor tissues administrated with anti-AQP3 mAbs were comparable to the control-IgG treatment (Fig. 2A, Supplementary Fig. 2B). The ratio of $CD8^+CD44^+CD62^-$ effector/memory type T cells (which attack tumor cells) to $CD45^+$ immune cells was higher in tissues administrated with anti-AQP3 mAbs compared to the control-IgG treatment (Fig. 2A). The mean fluorescence intensity (MFI) values of CD11C activation markers (CD80, MHCII) were unaffected by anti-AQP3 mAbs (Supplementary Fig. 2B).

Macrophages are generally categorized as either M1 or M2 subtypes based on MHCII and CD206 expression levels [9,38]. FACS analysis showed that there were more MHCII ^{high} $CD206^{low}$ M1-like TAMs and less MHCII ^{low} CD206 ^{high} M2-like TAMs in tumor tissue administered with anti-AQP3 mAbs compared to the control-IgG treatment (Fig. 2B). The ratio of M1- to M2-like TAMs increased significantly after anti-AQP3 mAb treatment (Fig. 2B). The ratios of monocytes to $CD45^+$immune cells in control-IgG and anti-AQP3 mAb treatments were comparable, suggesting that anti-AQP3 mAbs do not affect monocyte infiltration into tumor tissue (Fig. 2C).

M2-like TAMs suppress the proliferation of $CD8^+$ T cells, which results in immunosuppression [39]. Therefore, we determined the profiles of macrophages and effector/memory $CD8^+$T cells during the course of cancer progression. At 12 days after CT26 transplantation, the ratio of M1- to M2-like TAMs in the anti-AQP3 mAb treatment was significantly higher than that of the control-IgG treatment, while the number of $CD8^+$effector/memory T cells remained unchanged (Fig. 2D). The number of effector/memory type $CD8^+$ T cells in the anti-AQP3 mAb treatments increased significantly 22 days after CT26 transplantation, suggesting that anti-AQP3 mAb might affect macrophages before T cells.

It has been reported that exhausted T cells suppress mitochondrial respiration and impair anti-tumor immune responses in TME. Studies have shown that restoring T cell metabolism in draining lymph nodes is

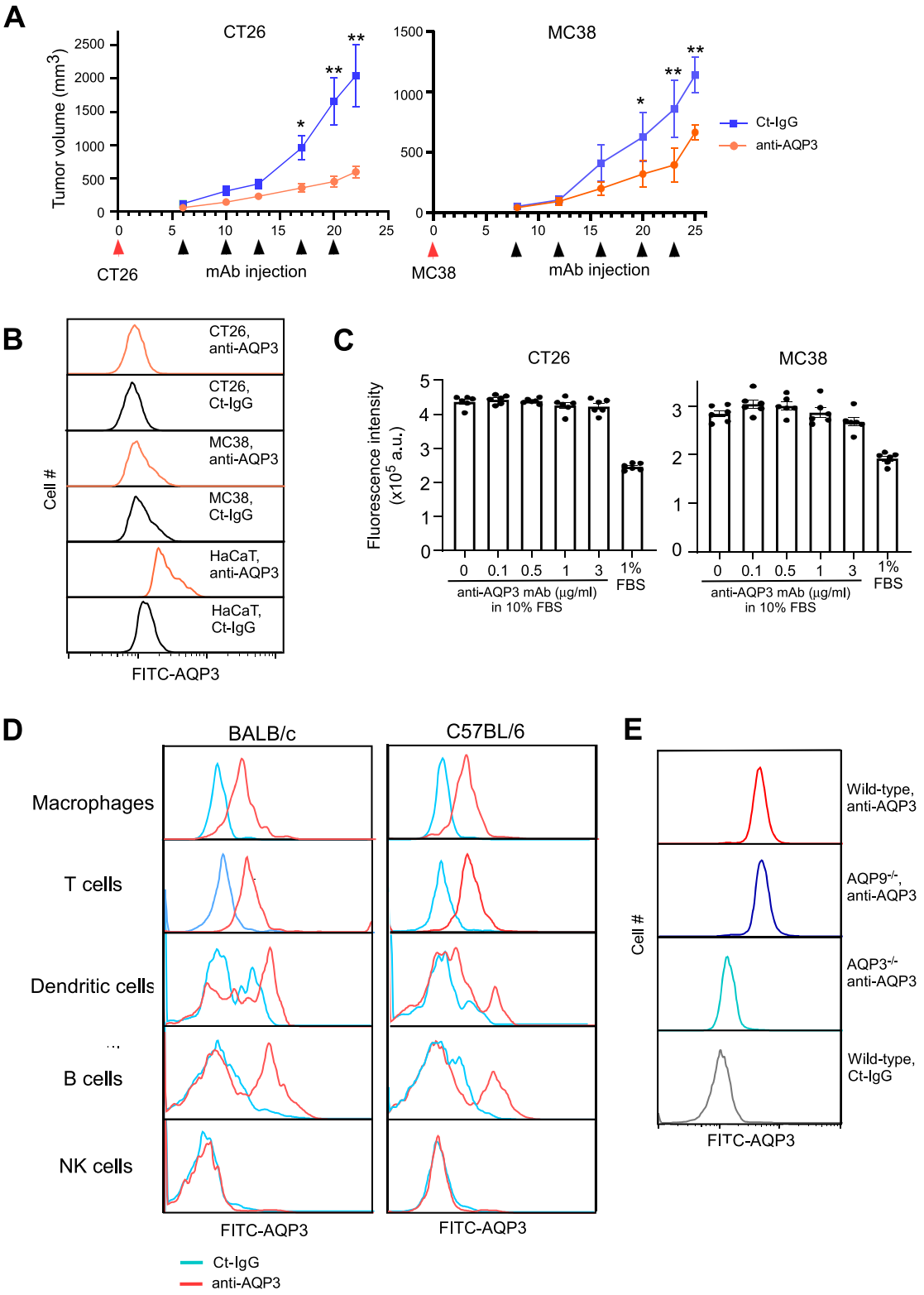

Fig. 1. *Anti-AQP3 mAb suppress tumor growth in a syngeneic mouse tumor model* **A.** BALB/c or C57BL/6 mice were injected with CT26 or MC38 colon carcinoma cells (4×10^6 cells in a 100 μl PBS) by intradermally at the right flank of mice. Anti-AQP3 mAb or mouse IgG2a isotype control (control-IgG) was injected intraperitoneally (12.5 mg/ kg weight, PBS) every 3 to 4 days. Tumor size was measured with digital caliper and calculated by the following formula: volume = (width^2 x length)/2 (mean ± SE, $n = 7$–8 mice/group, $^*p < 0.05$, $^{**}p < 0.01$ by two-way ANOVA with Sidak's multiple comparisons test). **B.** Binding of anti-AQP3 mAb and control-IgG to CT26, MC38, and HaCaT (as a positive control) by FACS analysis. **C.** CT26 and MC38 cells were cultured with anti-AQP3 mAb (0.1–3 μg/ml) in culture medium including 10% FBS. Culture with 1% FBS is negative control. Cell number was assessed by Cell Count Reagent SF kit (SE, $n = 6$). **D.** Binding of anti-AQP3 mAb and control-IgG to immune cells derived from BALB/c or C57BL/6 mice bone marrow or spleen by FACS analysis. **E.** Binding of anti-AQP3 mAb to macrophages derived from wild-type, AQP9$^{-/-}$, or AQP3$^{-/-}$ mice by FACS analysis.

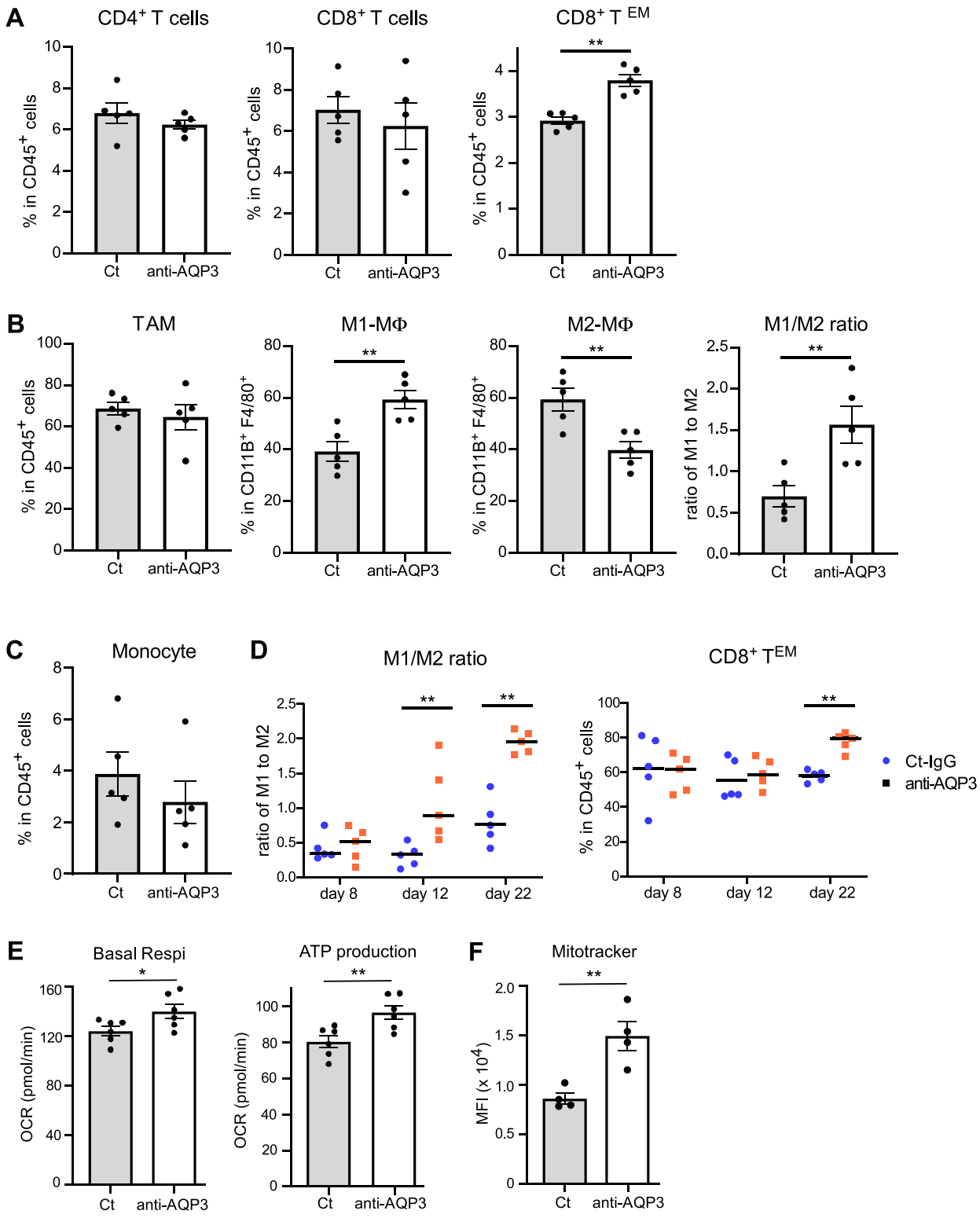

Fig. 2. *Administration of anti-AQP3 mAb alters intratumoral macrophage profile and T cell activation* **A–F.** BALB/c mice were injected with CT26 by intradermally. Anti-AQP3 mAb or mouse IgG2a isotype control (control-IgG) was injected intraperitoneally (12.5 mg/ kg weight, PBS) every 3 to 4 days as shown in Fig. 1A. **A–C.** Tumor tissues were collected at day 20 after transplantation and digested cells were analyzed by FACS (mean ± SE, $n = 5$ mice/group, $^{**}p < 0.01$). **D.** Tumor tissues were collected and analyzed at 8, 12, and 22 days after transplantation by FACS (mean ± SE, $n = 5$ mice/group, $^{**}p < 0.01$). **E. F.** T cells of draining lymph nodes were sorted by MACS. **E.** OCR was analyzed by Seahorse extracellular flux analyzer. Calculated basal respiration (left) and ATP production (right) (mean ± SE, $n = 6$, $^{*}p < 0.05$, $^{**}p < 0.01$). **F.** MFI of Mitotracker in T cells by FACS analysis (mean ± SE, $n = 4$, $^{**}p < 0.01$). Statistical analysis was performed by two-tailed unpaired Student *t*-test.

critical for effector functions and anti-tumor immunity [31,40–42]. Therefore, we determined mitochondrial activation using the extracellular Flux Analyzer™ and flow cytometry. Fig. 2E shows that $CD8^+$ T cells from the draining lymph node of anti-AQP3 mAb-treated mice had significantly higher levels of basal respiration and ATP production compared to those of the control-IgG treatment. FACS analysis also show that the MFI of mitochondrial membrane potential by MitoTracker™ is higher in $CD8^+$ T cell from anti-AQP3-treated mice than that in the control-IgG-treated mice (Fig. 2F).

These findings suggest that the administration of anti-AQP3 mAbs shifts the TAMs profile to one that is less immunosuppressive, *i.e.*, with a higher M1/M2 ratio, which consequently affects the mitochondrial function of T cells in the TME.

Anti-AQP3 mAb modulates the differentiation of monocytes to TAM

We investigated how anti-AQP3 mAbs affect the TAM profile by measuring the effect of anti-AQP3 mAb on macrophage polarization. We recently reported that LPS-induced M0 to M1 polarization is reduced in AQP3 knockout cells and in wild-type cells treated with anti-AQP3 mAbs. In contrast, IL-4 induced arginase 1 (Arg1) expression level, as marker for M2 polarization, was similar between wild-type and AQP3 knockout bone marrow-derived M0 macrophages [24]. Consistent with previous result, we verified that IL4-induced polarization of M0 to M2

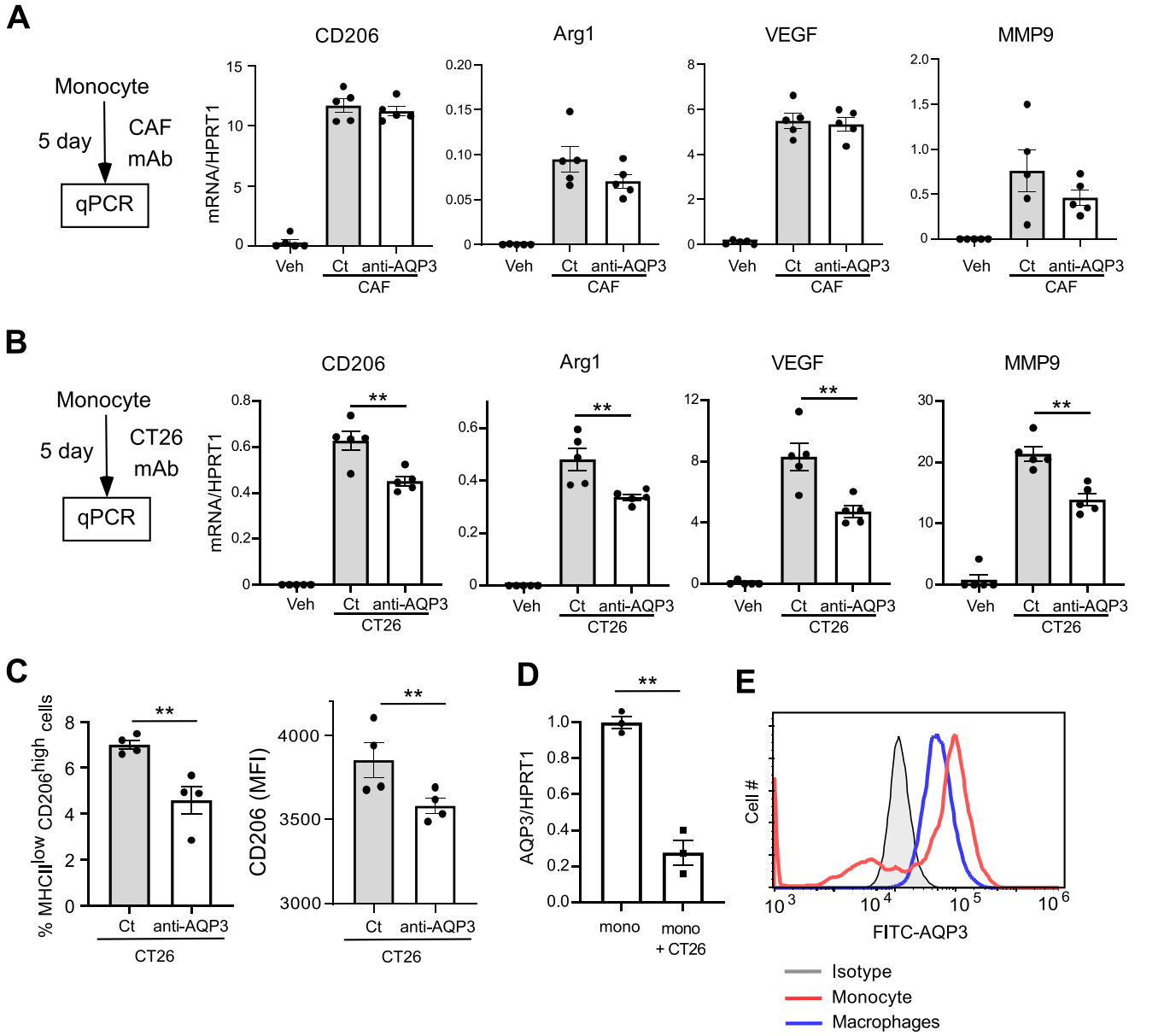

Fig. 3. *Anti-AQP3 mAb modulates the differentiation of monocytes to TAM* **A.** Monocytes were sorted from mice bone marrow cell suspension with MACS monocyte isolation kit. Tumor tissues were digested, and CAF were isolated with MACS tumor-associated fibroblast isolation kit. Monocytes were co-cultured with CAF using transwell for 5 days in the absence or presence of anti-AQP3 mAb (10 μg/ml). mRNA expression of indicated genes as the ratio to HPRT1 by real-time RT-PCR (mean ± SE, $n = 5$). **B–D.** Sorted monocytes were co-cultured with CT26 cancer cells using transwell for 5 days in the absence or presence of anti-AQP3 mAb (10 μg/ml). **B.** mRNA expression of indicated genes as the ratio to HPRT1 by real-time RT-PCR (mean ± SE, $n = 5$, $^{**}p < 0.01$ by two-way ANOVA with Tukey's multiple comparisons test.). **C.** Ratio of MHCII ^{low} CD206 ^{high} cells among $CD45^+$ cells (left) and mean fluorescence intensity (MFI) of $CD206^+$ cells (right) by FACS analysis (mean ± SE, $n = 4$, $^{**}p < 0.01$ by two-tailed unpaired Student *t*-test). **D.** mRNA expression of AQP3 as the ratio to HPRT1 by real-time RT-PCR in naïve monocytes or monocytes co-cultured with CT26 (mean ± SE, $n = 3$, $^{**}p < 0.01$ by two-tailed unpaired Student *t*-test). **E.** Flow cytometric analysis of binding of anti-AQP3 mAb to monocytes or macrophages. Representative FACS analysis.

type macrophages (characterized by the expression of CD206, Arg1, and CCL20) was not affected by anti-AQP3 mAb treatment (Supplementary Fig. 3A).

Monocytes are a major source of TAMs, which are the result of stromal cells recruiting monocytes from circulation and influencing their differentiation. The molecular basis for this differentiation is largely unknown [38,43,44]. Within the solid TME, cancer-associated fibroblast (CAF) and cancer cells were shown to influence TAM polarization [39,45,46]. Here, we investigated the effect of anti-AQP3 mAbs on the differentiation of monocytes into M2-like TAMs by CAF or cancer cells within a TME. First, we isolated naïve monocytes from bone marrow cells by magnetic activated cell sorting (MACS), and then we co-cultured the monocytes with CAF or CT26 cancer cells for 5 days. Both co-cultures expressed significantly higher levels of M2 TAMs markers (CD206, Arg1, VEGF, MMP9) than without co-culture, indicating that co-cultured monocytes had differentiated to M2-like TAMs (Fig. 3A, B). The supplementation of anti-AQP3 mAbs to the co-culture medium inhibited the cancer cell-induced polarization of monocytes into M2-like macrophages, while CAF-induced polarization was unaffected by anti-AQP3 (Fig. 3A, B). FACS analysis verified that the anti-AQP3 mAb reduced the cancer cell-induced levels of MHCII ^{low} CD206 ^{high} macrophages (a marker of M2-TAM) (Fig. 3C). Overall, these results show that anti-AQP3 mAbs suppress the cancer cell-induced differentiation of monocytes into M2-like TAMs. RT-PCR analysis show higher AQP3 expression levels in naïve monocytes than in cancer cell-induced TAM-like macrophages (Fig. 3D). Accordingly, FACS analysis shows that more anti-AQP3 mAbs bind to monocytes than to macrophages (Fig. 3E).

In addition, we sought to confirm the effect of anti-AQP3 mAb on monocyte polarization to TAM-like macrophages induced by cancer cells using the human monocyte cell line THP-1 cells. Previous studies showed that incubation of THP-1 cells with conditioned medium from human cancer cells, including breast or colon cancer cells, induced the differentiation of THP-1 monocytes into TAM-like macrophages [47,48]. THP-1 monocytes were cultured in conditioned medium from MDA-MB231 human breast cancer cells with or without anti-AQP3 mAb, and the expression levels of markers for TAMs were determined using real-time PCR (Fig. 4A) and FACS analysis (Fig. 4B). We found that supplementation of anti-AQP3 mAb suppressed the increase in cancer cell-mediated induction of markers for TAMs. These findings indicate that anti-AQP3 mAbs suppress cancer cell-mediated monocyte differentiation into M2-like TAM within the TME.

Anti-AQP3 mAbs suppress monocyte polarization and CD8$^+$ T cell proliferation in a murine syngeneic tumor model

We used a murine syngeneic tumor model to verify whether anti-AQP3 mAbs affect the polarization of monocytes into macrophages *in vivo*. Naïve monocytes were sorted from BALB/c mice bone marrow cells, stained using a Qtracker Cell Labeling kit™, and then transferred into CT26 tumor tissue (Fig. 5A, upper). Mice with CT26 cells were administrated either control-IgG or anti-AQP3 mAbs before and after

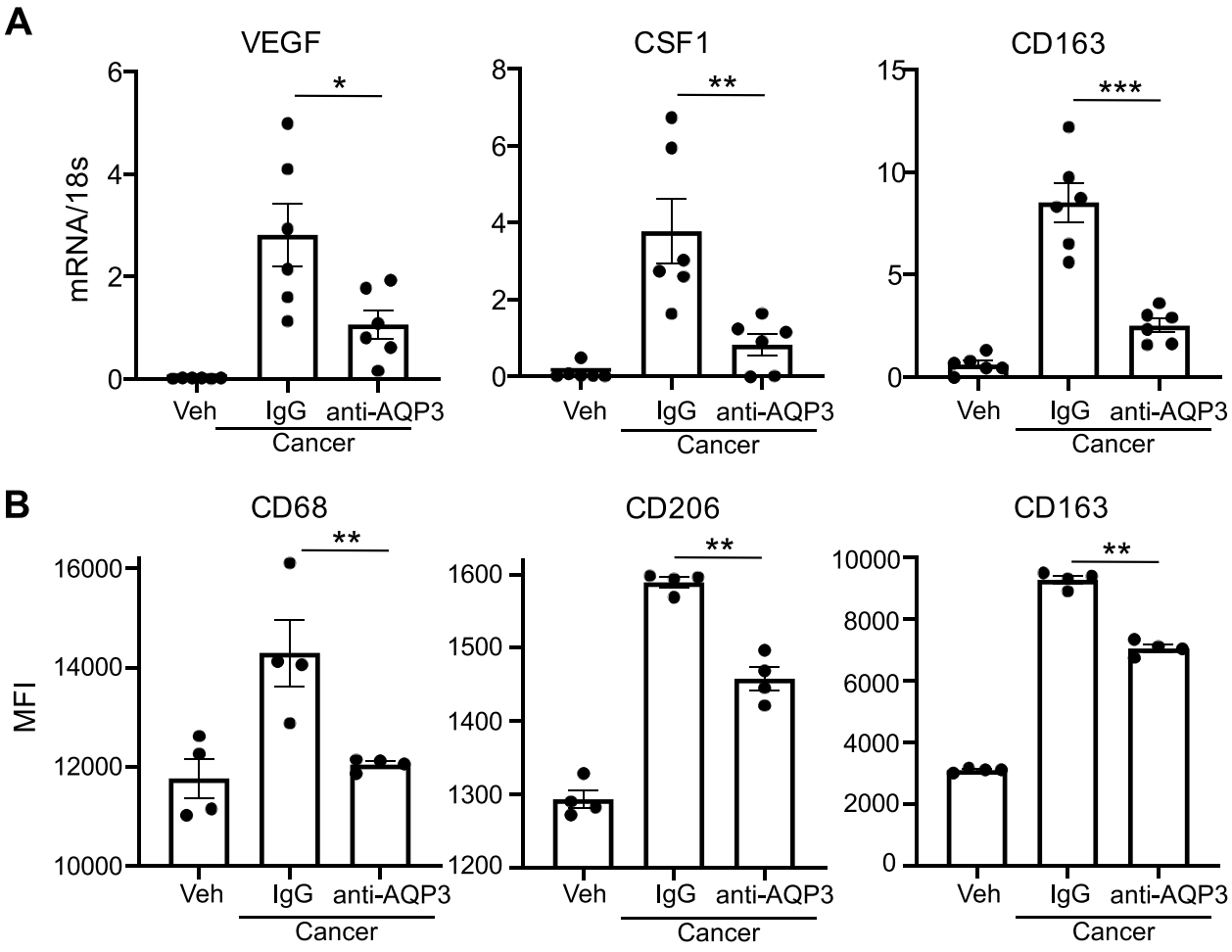

Fig. 4. *Anti-AQP3 mAb suppress cancer cell-induced differentiation of THP-1 monocytes* THP-1 monocyte cells were cultured with conditioned medium from MB-MDA231 cells for 4 days in the absence or presence of anti-AQP3 mAb (10 μg/ml). **A.** mRNA expression of indicated genes as the ratio to 18 s by real-time RT-PCR (mean ± SE, $n = 6$, *** $p < 0.001$, ** $p < 0.01$, * $p < 0.05$ by two-way ANOVA with Tukey's multiple comparisons test.). **B.** Mean fluorescence intensity (MFI) of CD68, CD206, and CD163 among CD11B$^+$ cells by FACS analysis (mean ± SE, $n = 4$, ** $p < 0.01$ by two-tailed unpaired Student *t*-test).

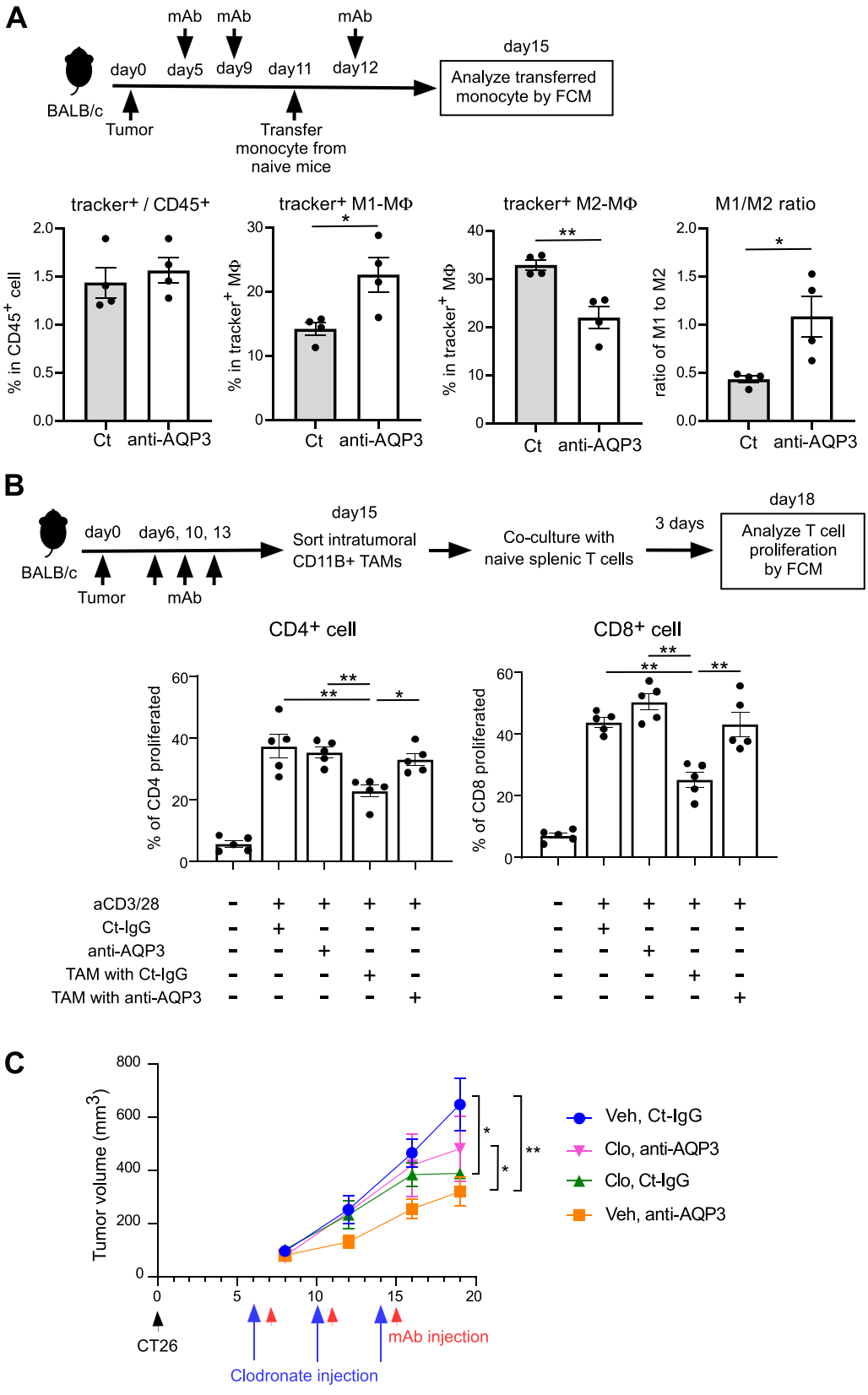

Fig. 5. *Anti-AQP3 mAb suppress monocyte polarization and CD8$^+$ T cell proliferation in a murine syngeneic tumor model* **A.** BALB/c mice were injected with CT26 cells (4×10^6 cells). Anti-AQP3 mAb or mouse IgG2a isotype control (control-IgG) was injected intraperitoneally (12.5 mg/ kg weight, PBS) at day 5, 9, and 12 after transplantation. Sorted monocytes from BALB/c mice bone marrow cells were stained with Qtracker Cell Labeling kit, and then transferred into CT26 tumor tissue at day 11. Tumor tissues were collected and analyzed at 4 days after transfer of monocytes by FACS (mean ± SE, $n = 4$ mice/group, $^*p < 0.05$, $^{**}p < 0.01$ by two-tailed unpaired Student *t*-test). **B.** BALB/c mice were injected with CT26 cells (4×10^6 cells). Anti-AQP3 mAb or mouse IgG2a isotype control (control-IgG) was injected intraperitoneally (12.5 mg/ kg weight, PBS) at day 6, 10, and 13 after transplantation. Splenic naïve T cells were sorted and stained with CFSE. Sorted CD11B$^+$ TAMs from tumor tissues were co-cultured with naïve T cells in the presence or absence of anti-CD3/28. Proliferative T cell was assessed by CFSE dilution using FACS analysis (mean ± SE, $n = 5$, $^*p < 0.05$, $^{**}p < 0.01$ by one-way ANOVA with Sidak's multiple comparisons test). **C.** BALB/c mice were injected with CT26 cells (4×10^6 cells). Clodronate liposome (Clo, 10 ml/kg) were injected intraperitoneally the day before antibody administrations. Anti-AQP3 mAb or mouse IgG2a isotype control (control-IgG) was injected intraperitoneally (12.5 mg/ kg weight, PBS) every 4 days. Tumor growth was measured (mean ± SE, $n = 6$ mice/group, $^*p < 0.05$, $^{**}p < 0.01$ by two-way ANOVA with Sidak's multiple comparisons test).

monocyte transfer. Four days after transplant, the tumor tissues were dissected and the macrophage profiles were analyzed by flow cytometry. The numbers of tracker-positive transferred cells in control-IgG- and anti-AQP3 mAb-treated mice were similar (Fig. 5A, left). There were more tracker-positive MHCII ^{high} CD206 ^{low} M1-like TAMs in anti-AQP3 mAb-treated mice than in the control treatment, while there were less MHCII ^{low} CD206 ^{high} M2-like TAMs in anti-AQP3 mAb-treated mice than in the control treatment. Therefore, the ratio of tracker-positive M1- to M2-like TAMs was significantly higher in the anti-AQP3 mAb-treated mice than in the control treatment (Fig. 5A, right). Overall, these

data show that anti-AQP3 mAbs suppress the polarization of monocytes into M2-like TAMs, while they promote the differentiation of monocytes into M1-like TAMs.

T cell proliferation is suppressed by TAMs, which leads to cancer progression [7,13,15]. Thus, we hypothesized that anti-AQP3 mAb can alleviated the decrease in T cell proliferation caused by TAM. To test this hypothesis, we isolated TAMs from tumor tissues that had been treated with control-IgG or anti-AQP3 mAbs, and then we co-cultured the TAMs with splenic naïve T cells. T cell proliferation was activated with anti-CD3/28 beads. The number of proliferated T cells (assessed by CFSE dilution and measured by FACS analysis) increased in response to CD3/28 stimulation. Co-culturing T cell with control TAMs suppressed the proliferation of $CD4^+$ and $CD8^+$ T cells, while TAMs from anti-AQP3 mAb-treated mice restored T cell proliferation (Fig. 5B), indicating that anti-AQP3 mAbs restore TAM-facilitated decrease in T cell function.

These data suggest that anti-AQP3 mAbs make M1 TAMs dominant over M2 TAMs in tumor tissues, and as a result, restores the impairment of T cell proliferation induced by M2-like TAMs.

Macrophage depletion suppresses the antitumoral effect of anti-AQP3 mAb

We next examined if the anti-AQP3 mAb shows an antitumoral effect by targeting macrophages. Mice were administered clodronate liposomes which deplete macrophages [49], and subsequent FACS analysis confirmed about 85% reduction in number of macrophages (Supplementary Fig. 4). Fig. 5C shows that administration of clodronate liposomes suppressed the growth of CT26-transferred tumor tissue. In mice administered with clodronate liposomes, the antitumoral effect of anti-AQP3 mAbs were counteracted, suggesting that macrophages are required for the antitumoral effect of AQP3 mAb.

Discussion

We have shown that an anti-AQP3 mAb suppresses primary tumor growth in two syngeneic murine cancer models (Fig. 1A). In detailed analysis of BALB/c mice cancer model with CT26 tumor, administration of an anti-AQP3 mAb increased the ratio of M1- to M2-like TAMs (Figs. 2B, D and 5A) as well as the proportion of effector/memory $CD8^+$ T cells with higher mitochondrial function in the TME (Fig. 2A, D–F). Results of time course analysis of tumoral immune cells show that anti-AQP3 mAbs first affect the TAM profile, followed by T cell effects (Fig. 2D). The efficacy of anti-AQP3 mAbs was abolished by depleting macrophages (Fig. 5C), indicating that the anti-AQP3 mAb affects primarily TAMs. Previous studies have indicated that M2-like TAMs attenuate the immunostimulatory function of T cells, resulting in immunosuppression of the TME [39,50]. Here, the administration of an anti-AQP3 mAb restored the TAM induced-suppression of T cell proliferation (Fig. 5B). In addition, *in vitro* studies with mice bone marrow derived cells and human monocyte cell line THP-1 showed that the anti-AQP3 mAb specifically suppressed cancer cell-induced differentiation of monocytes to M2-like macrophages (Figs. 3A–C and 4A, B). Although the molecular mechanism of how the anti-AQP3 mAb affects the TAM polarization remains unclear, our findings demonstrate that anti-AQP3 mAb alter the function of tumoral macrophages with predominantly immunostimulatory properties; and they enhance the T cell effector function in the TME, ultimately resulting in an antitumoral effect. On the other hand, previous studies have shown that the profile of infiltrated immune cells in the TME differs depending on the type of transplanted cancer cells, leading to the distinct mechanism of cancer progression [29–31]. Anti-AQP3 mAbs were found to be more effective in BALB/c mice with CT26 than in C57BL/6 mice with MC38; however, their mechanism of action for suppressing tumor growth might be different. Further studies are needed to define the mechanism of effectiveness according to cancer classification.

TAMs are an important therapeutic target to enhance the efficacy of immunotherapy [8,13]. Antitumor strategies targeting TAMs have focused mainly on depleting macrophages or inhibiting their recruitment into the TME; however, some of these strategies may cause unwanted side effects, such as increased susceptibility to infection [9]. Therefore, more reasonable approaches for anticancer therapy involves developing drugs to reprogram M2-like TAMs toward the antitumor M1 phenotype or shifting the M1/M2 TAM balance toward the antitumoral TAM phenotype [51,52]. In a solid TME, TAMs are thought to originate mostly from circulating monocytes, and they polarize to the M1 or M2 state depending on the environmental stimuli. However, the precise molecular mechanism of monocyte-to-macrophage differentiation in the TME is not fully understood [38,39,43,46]. Here, we show that an anti-AQP3 mAb reduces the differentiation of monocytes to M2-like macrophages, a process that is induced by carcinoma cells. The reduction produces a shift in the M1/M2 TAM balance toward the antitumoral TAM phenotype in mouse tumor model (Figs. 2B, 3B, C and 5A). Further studies are needed to establish the precise mechanism by which anti-AQP3 mAbs specifically inhibit the differentiation of monocyte into TAM induced by cancer cells. Such studies may lead to the identification of cancers that can be targeted by anti-AQP3 mAb therapy.

In summary, our findings indicate that anti-AQP3 mAb suppresses tumor growth in allograft mouse tumor models, and one of the underlying mechanisms of this effect is the attenuation of monocyte polarization into immunosuppressive M2-like TAMs. These findings thus suggest that anti-AQP3 mAbs are a potential cancer therapeutic approach that works by targeting TAM-mediated immune suppression followed by T cell-mediated immunosuppression within the TME.

Funding

This work was supported by Keio University Academic Development Funds (M.H-C), Keio Gijuku Fukuzawa Memorial Fund for the Advancement of Education (M.H-C), Research Ministry of Education, Culture, Sports, Science (21K06974, M.H-C), and Aqross Therapeutics, Inc.

CRediT authorship contribution statement

Manami Tanaka: Methodology, Data curation. **Anmi Ito:** Methodology, Data curation. **Seiji Shiozawa:** Visualization. **Mariko Hara-Chikuma:** Visualization, Methodology, Data curation, Writing – original draft.

Declaration of Competing Interest

The authors declare no competing financial interests.

Data Availability

Data will be made available on request.

Acknowledgments

We thank Dr. Masato Yasui for helpful discussion, and Mr. Gen Itai for generating AQP3 knockout mice. The generation of genome-edited mice was supported by the Laboratory Animal Center, Keio University School of Medicine.

Supplementary materials

Supplementary material associated with this article can be found, in the online version, at doi:10.1016/j.tranon.2022.101498.

References

[1] M.J. Bissell, W.C. Hines, Why do not we get more cancer? A proposed role of the microenvironment in restraining cancer progression, Nat. Med. 17 (2011) 320–329, https://doi.org/10.1038/nm.2328.

[2] D.F. Quail, J.A. Joyce, Microenvironmental regulation of tumor progression and metastasis, Nat. Med. 19 (2013) 1423–1437, https://doi.org/10.1038/nm.3394.

[3] S. Schworer, S.A. Vardhana, C.B. Thompson, Cancer metabolism drives a stromal regenerative response, Cell Metab. 29 (2019) 576–591, https://doi.org/10.1016/j.cmet.2019.01.015.

[4] M. Fane, A.T. Weeraratna, How the ageing microenvironment influences tumour progression, Nat. Rev. Cancer 20 (2020) 89–106, https://doi.org/10.1038/s41568-019-0222-9.

[5] S.K. Biswas, A. Mantovani, Macrophage plasticity and interaction with lymphocyte subsets: cancer as a paradigm, Nat. Immunol. 11 (2010) 889–896, https://doi.org/10.1038/ni.1937.

[6] F.O. Martinez, S. Gordon, The M1 and M2 paradigm of macrophage activation: time for reassessment, F1000Prime Rep. 6 (2014) 13, https://doi.org/10.12703/P6-13. http://f1000.com/prime/reports/b/6/1.

[7] L. Cassetta, T. Kitamura, Macrophage targeting: opening new possibilities for cancer immunotherapy, Immunology 155 (2018) 285–293, https://doi.org/10.1111/imm.12976.

[8] A.R. Poh, M. Ernst, Targeting macrophages in cancer: from bench to bedside, Front. Oncol. 8 (2018) 49, https://doi.org/10.3389/fonc.2018.00049.

[9] Y. Chen, Y. Song, W. Du, L. Gong, H. Chang, Z. Zou, Tumor-associated macrophages: an accomplice in solid tumor progression, J. Biomed. Sci. 26 (2019) 78, https://doi.org/10.1186/s12929-019-0568-z.

[10] K. Zhou, T. Cheng, J. Zhan, X. Peng, Y. Zhang, J. Wen, X. Chen, M. Ying, Targeting tumor-associated macrophages in the tumor microenvironment, Oncol. Lett. 20 (2020) 234, https://doi.org/10.3892/ol.2020.12097.

[11] C. Anfray, A. Ummarino, F.T. Andon, P. Allavena, Current strategies to target tumor-associated-macrophages to improve anti-tumor immune responses, Cells 9 (2019), https://doi.org/10.3390/cells9010046.

[12] X. Xiang, J. Wang, D. Lu, X. Xu, Targeting tumor-associated macrophages to synergize tumor immunotherapy, Signal Transduct. Target. Ther. 6 (2021) 75, https://doi.org/10.1038/s41392-021-00484-9.

[13] M. Lopez-Yrigoyen, L. Cassetta, J.W. Pollard, Macrophage targeting in cancer, Ann. N. Y. Acad. Sci. 1499 (2021) 18–41, https://doi.org/10.1111/nyas.14377.

[14] X. Geeraerts, E. Bolli, S.M. Fendt, J.A. Van Ginderachter, Macrophage metabolism as therapeutic target for cancer, Atheroscler. Obes. Front. Immunol. 8 (2017) 289, https://doi.org/10.3389/fimmu.2017.00289.

[15] L. Cassetta, T. Kitamura, Targeting tumor-associated macrophages as a potential strategy to enhance the response to immune checkpoint inhibitors, Front. Cell Dev. Biol. 6 (2018) 38, https://doi.org/10.3389/fcell.2018.00038.

[16] M. Hara-Chikuma, A.S. Verkman, Aquaporin-3 facilitates epidermal cell migration and proliferation during wound healing, J. Mol. Med. 86 (2008) 221–231, https://doi.org/10.1007/s00109-007-0272-4 (Berl).

[17] M. Hara-Chikuma, A.S. Verkman, Roles of aquaporin-3 in the epidermis, J. Invest. Dermatol. 128 (2008) 2145–2151, https://doi.org/10.1038/jid.2008.70.

[18] M. Hara-Chikuma, A.S. Verkman, Prevention of skin tumorigenesis and impairment of epidermal cell proliferation by targeted aquaporin-3 gene disruption, Mol. Cell. Biol. 28 (2008) 326–332, https://doi.org/10.1128/MCB.01482-07.

[19] A.S. Verkman, M.O. Anderson, M.C. Papadopoulos, Aquaporins: important but elusive drug targets, Nat. Rev. Drug Discov. 13 (2014) 259–277, https://doi.org/10.1038/nrd4226.

[20] K. Nakahigashi, K. Kabashima, A. Ikoma, A.S. Verkman, Y. Miyachi, M. Hara-Chikuma, Upregulation of aquaporin-3 is involved in keratinocyte proliferation and epidermal hyperplasia, J. Investig. Dermatol. 131 (2011) 865–873, https://doi.org/10.1038/jid.2010.395.

[21] M. Hara-Chikuma, S. Chikuma, Y. Sugiyama, K. Kabashima, A.S. Verkman, S. Inoue, Y. Miyachi, Chemokine-dependent T cell migration requires aquaporin-3-mediated hydrogen peroxide uptake, J. Exp. Med. 209 (2012) 1743–1752, https://doi.org/10.1084/jem.20112398.

[22] K. Ikezoe, T. Oga, T. Honda, M. Hara-Chikuma, X. Ma, T. Tsuruyama, K. Uno, J. Fuchikami, K. Tanizawa, T. Handa, Y. Taguchi, A.S. Verkman, S. Narumiya, M. Mishima, K. Chin, Aquaporin-3 potentiates allergic airway inflammation in ovalbumin-induced murine asthma, Sci. Rep. 6 (2016) 25781, https://doi.org/10.1038/srep25781.

[23] M. Hara-Chikuma, H. Satooka, S. Watanabe, T. Honda, Y. Miyachi, T. Watanabe, A. S. Verkman, Aquaporin-3-mediated hydrogen peroxide transport is required for NF-kappaB signalling in keratinocytes and development of psoriasis, Nat. Commun. 6 (2015) 7454, https://doi.org/10.1038/ncomms8454.

[24] M. Hara-Chikuma, M. Tanaka, A.S. Verkman, M. Yasui, Inhibition of aquaporin-3 in macrophages by a monoclonal antibody as potential therapy for liver injury, Nat. Commun. 11 (2020) 5666, https://doi.org/10.1038/s41467-020-19491-5.

[25] H. Satooka, M. Hara-Chikuma, Aquaporin-3 controls breast cancer cell migration by regulating hydrogen peroxide transport and its downstream cell signaling, Mol. Cell. Biol. 36 (2016) 1206–1218, https://doi.org/10.1128/MCB.00971-15.

[26] M. Hara-Chikuma, S. Watanabe, H. Satooka, Involvement of aquaporin-3 in epidermal growth factor receptor signaling via hydrogen peroxide transport in cancer cells, Biochem. Biophys. Res. Commun. 471 (2016) 603–609, https://doi.org/10.1016/j.bbrc.2016.02.010.

[27] A.M. Rojek, M.T. Skowronski, E.M. Fuchtbauer, A.C. Fuchtbauer, R.A. Fenton, P. Agre, J. Frokiaer, S. Nielsen, Defective glycerol metabolism in aquaporin 9 (AQP9) knockout mice, Proc. Natl. Acad. Sci. USA 104 (2007) 3609–3614, https://doi.org/10.1073/pnas.0610894104.

[28] T. Clackson, H.R. Hoogenboom, A.D. Griffiths, G. Winter, Making antibody fragments using phage display libraries, Nature 352 (1991) 624–628, https://doi.org/10.1038/352624a0.

[29] M.G. Lechner, S.S. Karimi, K. Barry-Holson, T.E. Angell, K.A. Murphy, C.H. Church, J.R. Ohlfest, P. Hu, A.L. Epstein, Immunogenicity of murine solid tumor models as a defining feature of *in vivo* behavior and response to immunotherapy, J. Immunother. 36 (2013) 477–489, https://doi.org/10.1097/01.cji.0000436722.46675.4a.

[30] S.I. Mosely, J.E. Prime, R.C. Sainson, J.O. Koopmann, D.Y. Wang, D.M. Greenawalt, M.J. Ahdesmaki, R. Leyland, S. Mullins, L. Pacelli, D. Marcus, J. Anderton, A. Watkins, J. Coates Ulrichsen, P. Brohawn, B.W. Higgs, M. McCourt, H. Jones, J. A. Harper, M. Morrow, V. Valge-Archer, R. Stewart, S.J. Dovedi, R.W. Wilkinson, Rational selection of syngeneic preclinical tumor models for immunotherapeutic drug discovery, Cancer Immunol. Res. 5 (2017) 29–41, https://doi.org/10.1158/2326-6066.CIR-16-0114.

[31] A. Kumar, K. Chamoto, P.S. Chowdhury, T. Honjo, Tumors attenuating the mitochondrial activity in T cells escape from PD-1 blockade therapy, eLife 9 (2020) e52330, https://doi.org/10.7554/eLife.52330.

[32] A. de Baey, A. Lanzavecchia, The role of aquaporins in dendritic cell macropinocytosis, J. Exp. Med. 191 (2000) 743–748, https://doi.org/10.1084/jem.191.4.743.

[33] S. Watanabe, C.S. Moniaga, S. Nielsen, M. Hara-Chikuma, Aquaporin-9 facilitates membrane transport of hydrogen peroxide in mammalian cells, Biochem. Biophys. Res. Commun. 471 (2016) 191–197, https://doi.org/10.1016/j.bbrc.2016.01.153.

[34] C.S. Moniaga, S. Watanabe, T. Honda, S. Nielsen, M. Hara-Chikuma, Aquaporin-9-expressing neutrophils are required for the establishment of contact hypersensitivity, Sci. Rep. 5 (2015) 15319, https://doi.org/10.1038/srep15319.

[35] I. Vitale, G. Manic, L.M. Coussens, G. Kroemer, L. Galluzzi, Macrophages and metabolism in the tumor microenvironment, Cell Metab. 30 (2019) 36–50, https://doi.org/10.1016/j.cmet.2019.06.001.

[36] D.G. DeNardo, B. Ruffell, Macrophages as regulators of tumour immunity and immunotherapy, Nat. Rev. Immunol. 19 (2019) 369–382, https://doi.org/10.1038/s41577-019-0127-6.

[37] J.S. O'Donnell, M.W.L. Teng, M.J. Smyth, Cancer immunoediting and resistance to T cell-based immunotherapy, Nat. Rev. Clin. Oncol. 16 (2019) 151–167, https://doi.org/10.1038/s41571-018-0142-8.

[38] K. Movahedi, J.A. Van Ginderachter, The ontogeny and microenvironmental regulation of tumor-associated macrophages, Antioxid. Redox Signal. 25 (2016) 775–791, https://doi.org/10.1089/ars.2016.6704.

[39] S. Devalaraja, T.K.J. To, I.W. Folkert, R. Natesan, M.Z. Alam, M. Li, Y. Tada, K. Budagyan, M.T. Dang, L. Zhai, G.P. Lobel, G.E. Ciotti, T.S.K. Eisinger-Mathason, I.A. Asangani, K. Weber, M.C. Simon, M. Haldar, Tumor-derived retinoic acid regulates intratumoral monocyte differentiation to promote immune suppression, Cell 180 (2020) 1098–1114, https://doi.org/10.1016/j.cell.2020.02.042, e1016.

[40] M.D. Buck, D. O'Sullivan, R.I. Klein Geltink, J.D. Curtis, C.H. Chang, D.E. Sanin, J. Qiu, O. Kretz, D. Braas, G.J. van der Windt, Q. Chen, S.C. Huang, C.M. O'Neill, B. T. Edelson, E.J. Pearce, H. Sesaki, T.B. Huber, A.S. Rambold, E.L. Pearce, Mitochondrial dynamics controls T cell fate through metabolic programming, Cell 166 (2016) 63–76, https://doi.org/10.1016/j.cell.2016.05.035.

[41] N.M. Chapman, M.R. Boothby, H. Chi, Metabolic coordination of T cell quiescence and activation, Nat. Rev. Immunol. 20 (2020) 55–70, https://doi.org/10.1038/s41577-019-0203-y.

[42] Y. Guo, Y.Q. Xie, M. Gao, Y. Zhao, F. Franco, M. Wenes, I. Siddiqui, A. Bevilacqua, H. Wang, H. Yang, B. Feng, X. Xie, C.M. Sabatel, B. Tschumi, A. Chaiboonchoe, Y. Wang, W. Li, W. Xiao, W. Held, P. Romero, P.C. Ho, L. Tang, Metabolic reprogramming of terminally exhausted CD8(+) T cells by IL-10 enhances anti-tumor immunity, Nat. Immunol. 22 (2021) 746–756, https://doi.org/10.1038/s41590-021-00940-2.

[43] V. Cortez-Retamozo, M. Etzrodt, A. Newton, P.J. Rauch, A. Chudnovskiy, C. Berger, R.J. Ryan, Y. Iwamoto, B. Marinelli, R. Gorbatov, R. Forghani, T.I. Novobrantseva, V. Koteliansky, J.L. Figueiredo, J.W. Chen, D.G. Anderson, M. Nahrendorf, F. K. Swirski, R. Weissleder, M.J. Pittet, Origins of tumor-associated macrophages and neutrophils, Proc. Natl. Acad. Sci. USA 109 (2012) 2491–2496, https://doi.org/10.1073/pnas.1113744109.

[44] C.E. Olingy, H.Q. Dinh, C.C. Hedrick, Monocyte heterogeneity and functions in cancer, J. Leukoc. Biol. 106 (2019) 309–322, https://doi.org/10.1002/JLB.4RI0818-311R.

[45] X. Chen, E. Song, Turning foes to friends: targeting cancer-associated fibroblasts, Nat. Rev. Drug Discov. 18 (2019) 99–115, https://doi.org/10.1038/s41573-018-0004-1.

[46] H. Salmon, R. Remark, S. Gnjatic, M. Merad, Host tissue determinants of tumour immunity, Nat. Rev. Cancer 19 (2019) 215–227, https://doi.org/10.1038/s41568-019-0125-9.

[47] K. Sawa-Wejksza, A. Dudek, M. Lemieszek, K. Kalawaj, M. Kandefer-Szerszen, Colon cancer-derived conditioned medium induces differentiation of THP-1 monocytes into a mixed population of M1/M2 cells, Tumour Biol. 40 (2018), 1010428318797880, https://doi.org/10.1177/1010428318797880.

[48] Y.H. Wang, C.Y. Shen, S.C. Lin, W.H. Kuo, Y.T. Kuo, Y.L. Hsu, W.C. Wang, K.T. Lin, L.H. Wang, Monocytes secrete CXCL7 to promote breast cancer progression, Cell Death. Dis. 12 (2021) 1090, https://doi.org/10.1038/s41419-021-04231-4.

[49] N. Van Rooijen, A. Sanders, Liposome mediated depletion of macrophages: mechanism of action, preparation of liposomes and applications, J. Immunol. Methods 174 (1994) 83–93.

[50] D.S. Chen, I. Mellman, Oncology meets immunology: the cancer-immunity cycle, Immunity 39 (2013) 1–10, https://doi.org/10.1016/j.immuni.2013.07.012.
[51] C.W. Wanderley, D.F. Colon, J.P.M. Luiz, F.F. Oliveira, P.R. Viacava, C.A. Leite, J. A. Pereira, C.M. Silva, C.R. Silva, R.L. Silva, C.A. Speck-Hernandez, J.M. Mota, J. C. Alves-Filho, R.C. Lima-Junior, T.M. Cunha, F.Q. Cunha, Paclitaxel reduces tumor growth by reprogramming tumor-associated macrophages to an M1 profile in a TLR4-dependent manner, Cancer Res. 78 (2018) 5891–5900, https://doi.org/10.1158/0008-5472.CAN-17-3480.
[52] J. Kowal, M. Kornete, J.A. Joyce, Re-education of macrophages as a therapeutic strategy in cancer, Immunotherapy 11 (2019) 677–689, https://doi.org/10.2217/imt-2018-0156.